

Hilbert transform, Gabor deconvolution and phase corrections

Carlos A. Montaña and Gary F. Margrave

ABSTRACT

Constant Q theory is a simple and robust theoretical model for seismic waves attenuation which needs just two parameters to characterize anelastic attenuation in a medium: the quality factor Q and a reference frequency ω_0 , for which the phase velocity is known. The convolutional model for a seismic trace can be extended to nonstationary attenuated traces using the constant- Q theory. Gabor deconvolution is a nonstationary extension of Wiener's deconvolution by factorizing the attenuated trace with the help of the Gabor transform. Both deconvolution methods are based on minimum phase assumptions and make use of the Hilbert transform for estimating the phase spectrum of the deconvolution operator. Gabor deconvolution compensates for the amplitude losses due to attenuation without necessity of any estimation of Q . However time shift and phase rotations between a recorded seismic trace and a synthetic trace generated from a well log remains after Gabor deconvolution is applied. One of the main causes of these phase differences is the fact that the digital Hilbert transform is an imperfect estimation of the analytical Hilbert transform. The phase shift can be removed partially either by adding a function, linear in time and quadratic in frequency, to the digital Hilbert transform estimation of the minimum phase function of the Gabor deconvolution operator or, by resampling the trace to a smaller sample rate.

INTRODUCTION

Gabor deconvolution is an extension of the stationary Wiener's deconvolution algorithm to apply nonstationary deconvolution. Wiener's algorithm posed in the Fourier domain is generalized by using a nonstationary extension of the Fourier transform such as the Gabor transform (Margrave et al, 2005). Gabor deconvolution is an alternate method to inverse- Q filter to compensate for attenuation effects. Although both methods use the constant- Q theory (Kjartansson, 1979) as a background theoretical model to represent attenuation there are essential differences between them. In inverse- Q filtering, the seismic data are compensated for attenuation effects before dealing with the inversion of the minimum-phase earth filter by spiking deconvolution. Theoretically, this ordering is incorrect. Gabor deconvolution approaches the compensation for attenuation in a radically different way, compensating for attenuation effects and inverting the minimum-phase earth wavelet simultaneously. Although this difference in methodology for tackling the attenuation problem defines already an important distinction between the two methods, there is one additional even more important difference: an estimation of Q is necessary for applying an inverse- Q filter, whereas to apply Gabor deconvolution knowledge of Q is not required. However it is necessary to observe at this point that the performance of Gabor deconvolution can be improved in relation to the phase problems discussed in this paper if an estimation of Q is available.

The nonstationary convolution model for the seismic trace considers the attenuated trace as the convolution between a minimum phase wavelet and a pseudodifferential operator which symbol is a minimum phase time-frequency attenuation function, applied

on the reflectivity (Margrave et al., 2005). Assuming that the wavelet has the minimum phase characteristic is a fundamental element both in Wiener and In Gabor deconvolution. Minimum phase means that the wavelet has the least possible phase delay among all causal invertible wavelets with the same amplitude spectrum (Robinson and Treitel, 1980). In signal theory a minimum phase wavelet is also defined as a causal stable wavelet with a causal stable inverse, in which the term ‘stable’ is associated with a precise physical meaning: finite energy. An additional step forward into the mathematical theory of minimum phase wavelets allows to come across an extraordinary, interesting and useful result: in a minimum phase wavelet its phase spectrum is equal to the Hilbert transform of the logarithm of its amplitude spectrum. Given the fact that nature seems to like minimum phase, there are several physical processes which are suspected to have this attribute, although just approximately since no physical system can radiate at all frequencies from zero to infinity. There are two of such processes in seismic theory: the wavelet signature of an explosive source and the anelastic attenuation earth filter suffered by the seismic waves traveling through the earth interior. The constant Q model for attenuation gives a theoretical support to the minimum phase attenuation hypothesis that attenuation is a minimum phase process. Gabor deconvolution is based on the constant Q theory, therefore the Gabor deconvolution operator has minimum phase characteristics.

Mathematics gives an elegant frame and a very precise tool to compute the phase of a minimum phase operator: the Hilbert transform. However what is exact and robust in the theoretical mathematical universes, turns out not to be so good in the real word on which the seismic waves are propagated, recorded and processed. In particular the mathematical definition of the Hilbert transform is formulated for continuous functions, which frequency spectrum can be known over a range of frequencies extending to the infinity. In contrast, the recorded seismic signal is discrete, and generally recorded using a finite sample rate that imposes a limit in the maximum accessible frequency, the Nyquist frequency. In the ideal world of the continuous finite length functions (analytic), consequently with infinite frequency spectrum, the analytic Hilbert transform is a unique function. However the real-world signals are bandlimited, which has as consequence that its digital Hilbert transform be different from its corresponding analytical Hilbert transform, and besides be dependent on two practical parameters: the Nyquist frequency and the stabilization factor. This factor is used to avoid finding zeros in the amplitude spectrum, for which the natural logarithm is not defined.

The purpose of this work is to analyze the impact of the Hilbert transform dependence on the Nyquist frequency and the stabilization factor and the influence of this dependence in Gabor deconvolution. Since it is the phase component of the deconvolution operator which is estimated through the digital Hilbert transform, the phase spectrum of the deconvolved signal is affected. The effects of inaccuracies in the phase spectrum are perceived in the signal as phase rotations (change in the shape of the events) or time shifts (event delays). As normally the two effects appear combined it is necessary to track them separately.

It will be shown that the difference between the analytic and the digital Hilbert transform, and the dependence of the latter on the sample rate and the stabilization factor, is responsible for some of the phase-shifts and phase-rotations appeared in the process of

tying deconvolved seismic data with synthetic traces generated from well logs. A partial correction of these effects can be achieved by applying a correction term to the estimation of the digital Hilbert transform.

THEORY

Modeling attenuation, the constant Q model

A nonstationary convolutional model for an attenuated seismic trace, s , can be derived from the constant- Q theory by applying the forward Q filter, as a pseudodifferential operator, to a reflectivity function and then by convolving the result with a minimum phase wavelet. Such a model has been used, for example by Margrave et al. (2005), and can be expressed in the frequency domain,

$$\hat{s}(\omega) = \frac{1}{2\pi} \hat{w}(\omega) \int_{-\infty}^{\infty} \alpha_Q(\omega, \tau) r(\tau) e^{i\omega(t-\tau)} d\tau. \quad (1)$$

where the ‘hat’ symbol indicates the Fourier transform, ω is the frequency, r is the reflectivity function, w is the wavelet and $\alpha_Q(\omega, \tau)$ is the time-frequency exponential attenuation function, defined as

$$\alpha_Q(\omega, \tau) = \exp(-\omega\tau/2Q + iH(\omega\tau/2Q)). \quad (2)$$

in which the real and imaginary components in the exponent and connected through the Hilbert transform H , result that is consistent with the minimum phase characteristic associated with the attenuated pulse. As written, equation (1) assumes a spatially constant Q and models only primaries though both of these simplifications can be removed with a slight complication in the formula.

Gabor deconvolution

The Gabor transform, G , maps functions of time to complex-valued functions of time and frequency using a windowed Fourier transform. Gabor deconvolution is a nonstationary extension of Wiener’s deconvolution method, based on an approximate, asymptotic factorization of the nonstationary trace model of equation (1)

$$Gs(t, \omega) \approx \hat{w}(\omega) \alpha_Q(t, \omega) Gr(t, \omega), \quad (3)$$

which states that the Gabor transform of the seismic trace, $Gs(t, \omega)$, is approximately equal to the product of the Fourier transform of the source wavelet, $\hat{w}(\omega)$, the time-frequency attenuation function, $\alpha_Q(t, \omega)$, and the Gabor transform of the reflectivity $Gr(t, \omega)$. The method assumes that $|Gr(t, \omega)|$ is a rapidly varying function in both variables τ and ω , $|\hat{w}(\omega)|$ is smoothly varying in ω and $\alpha_Q(t, \omega)$ is an exponentially decaying function in both variables τ and ω , and constant over hyperbolic families of $\tau\omega = \text{constant}$. Analogously to the Wiener’s method, Gabor deconvolution smoothes the Gabor magnitude spectrum of the seismic signal $|Gs(t, \omega)|$ to estimate the product of the magnitudes of the attenuation function and the source signature

$$|\sigma(t, \omega)| = |\hat{w}(\omega)| |\alpha_Q(t, \omega)|. \quad (4)$$

A phase function for $\sigma(t, \omega)$ is then estimated, with the help of the digital Hilbert transform, H , using the minimum phase assumption,

$$\varphi(t, \omega) = H(\ln|\sigma(t, \omega)|) \quad (5)$$

where the digital Hilbert transform is taken over frequency. Finally the Gabor spectrum of the reflectivity is estimated in the Gabor domain as:

$$Gr(t, \omega)_{est} = \frac{Gs(t, \omega)}{\sigma(t, \omega)} \quad (6)$$

and the reflectivity estimate is then recovered as the inverse Gabor transform of the result of equation (6).

Estimating phase differences

Modifications of the phase spectrum of a signal result in transformations of the signal which can result in time shifts as in figure 1, angle rotations (change in the shape of the event) as in figure 2, or more generally in a combination of both effects as in figure 3.

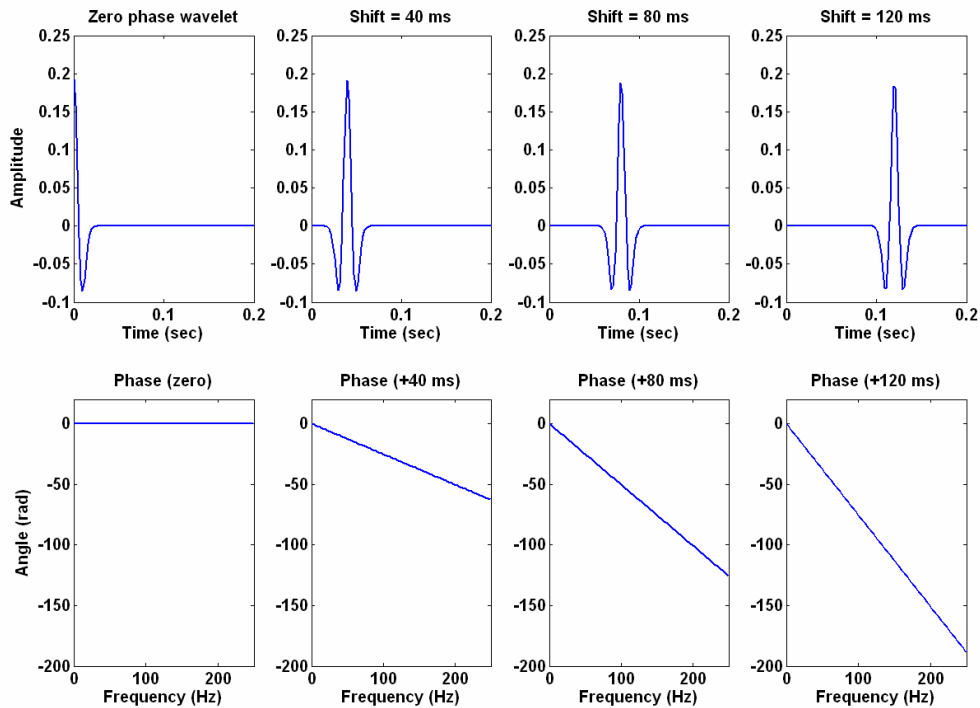


FIG 1. A wavelet and its phase spectrum for different time shifts. The slope of the phase spectrum is proportional to the time shift applied. The four wavelets have the same amplitude spectrum.

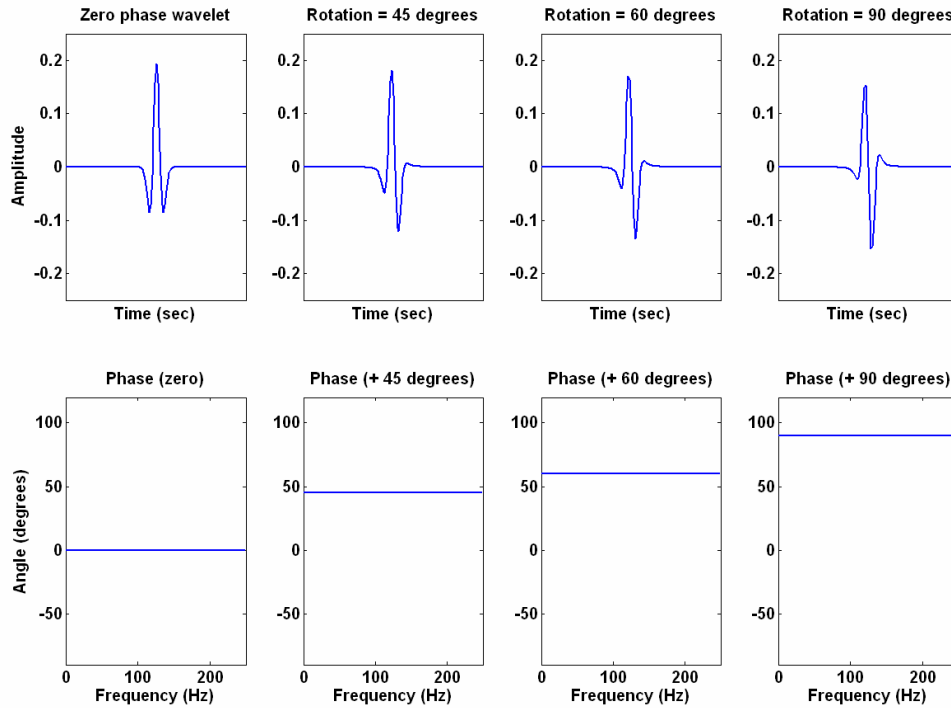


FIG. 2. A zero phase wavelet and its corresponding phase spectrum after applying a rotation for different angles. The four wavelets have the same amplitude spectrum.

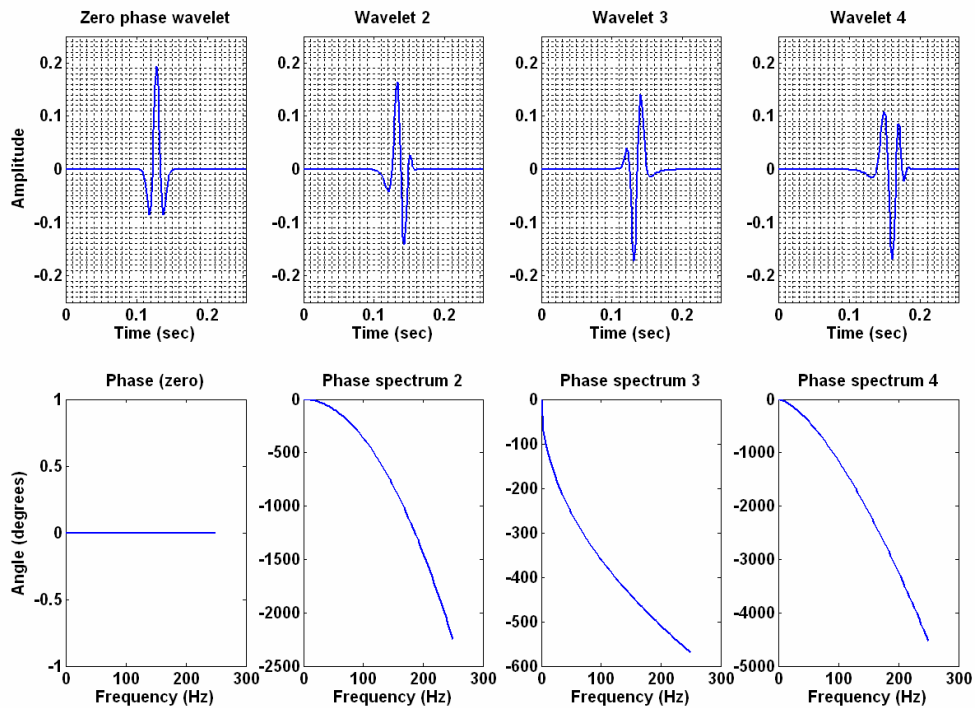


FIG. 3. A zero phase wavelet and three equivalent wavelets with different phase spectra. A combined effect of time shifting and rotation can be observed. The four wavelets have the same amplitude spectrum.

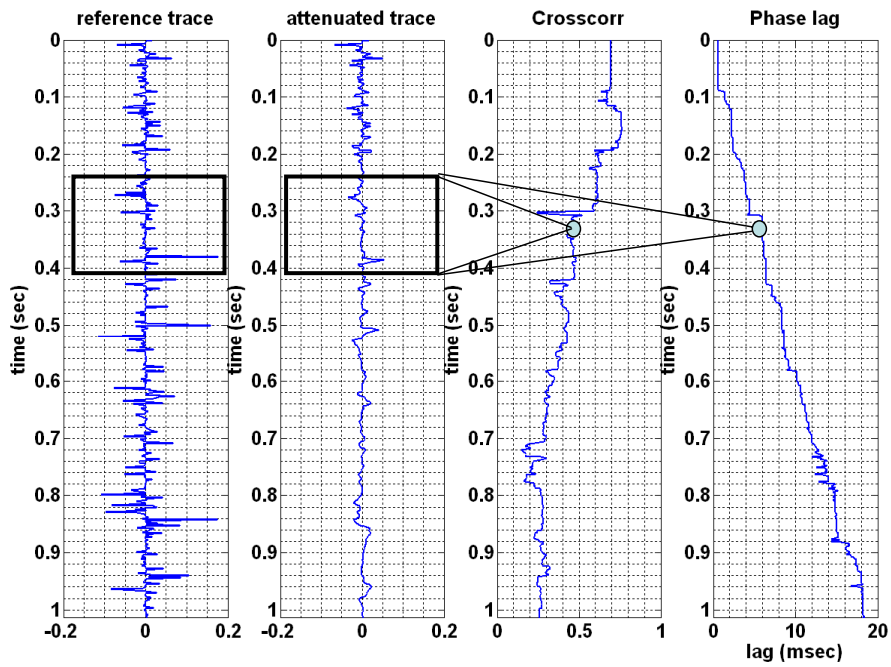


FIG. 4. Phase lag estimation. The difference in phase between 2 traces is estimated by the windowed crosscorrelation. The maximum coefficient of the crosscorrelation and its lag indicate similarity and phase lag respectively, for the middle point of the window.

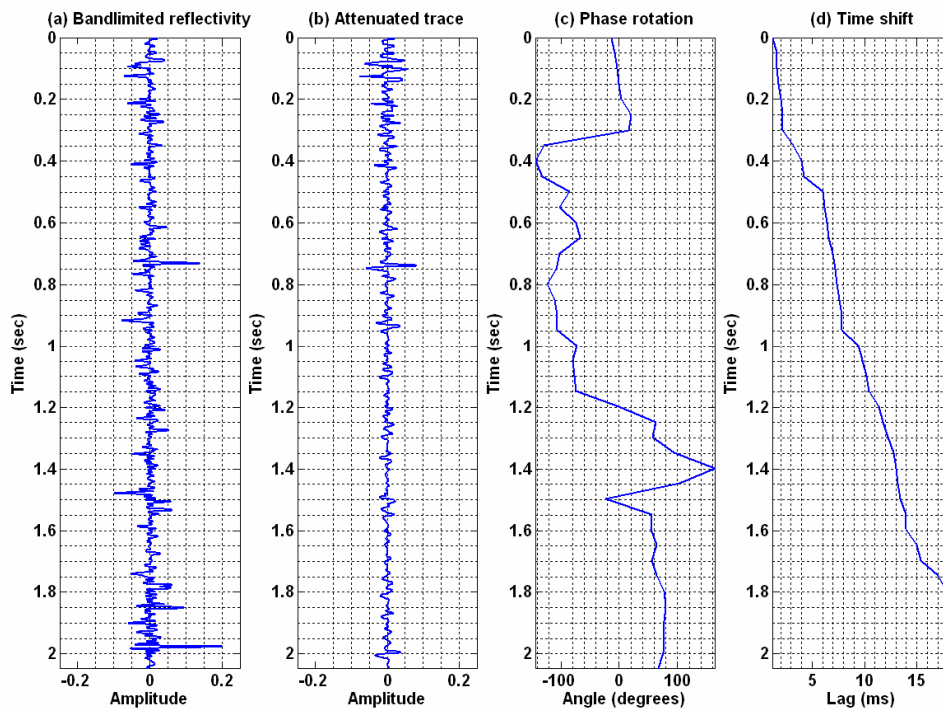


FIG. 5. An evaluation of the phase differences between two signals can be obtained by computing time-variant phase rotations and time shifts. (a): Bandlimited synthetic reflectivity. (b): Synthetic attenuated trace created by applying a forward Q filter to the reflectivity and then convolving the result with a minimum phase wavelet. (c): Time-variant phase rotation between (a) and (b). (d): Time shift between (a) and (b).

An estimation of the time shift and the phase rotation can be achieved by using trace attributes. The lag of the maximum coefficient of the crosscorrelation between two signals can be interpreted as a measure of the time shift. For the phase rotation, an angle can be estimated by minimizing the L2 norm of the difference between one signal and the other rotated by a constant angle. The nonstationarity introduced by attenuation can be handled by estimating the attributes on the windowed signals. By shifting the window along the signal a time-variant characterization of the phase differences can be generated as shown in figure 4 and 5.

Analytic vs. Digital Hilbert transform

The estimation of the phase spectrum of the Gabor deconvolution operator is achieved by resorting to the minimum phase assumption through the Hilbert transform. This phase delay is determined by the Hilbert transform of a function of frequency and can be found either analytically, by using Equation (9), or digitally, by using the definition of the Hilbert transform,

$$H\left(\frac{\omega\tau}{2Q}\right) = \frac{1}{\pi} \int_{-\infty}^{\infty} \frac{\frac{\omega'\tau}{2Q}}{\omega' - \omega} d\omega'. \quad (7)$$

To compute the phase delay from the definition given to the Hilbert transform in Equation (7), a corresponding finite discrete definition must be used,

$$H\left(\frac{\omega\tau}{2Q}\right) = \frac{1}{\pi} \sum_{n=-N}^N \frac{\frac{\omega_n\tau}{2Q}}{\omega_n - \omega} \Delta\omega. \quad (8)$$

The digital method to compute the phase, using Equation (8), has the disadvantage of substituting the infinite limits in the definition of the Hilbert transform with finite limits determined by the sample rate. An error in the phase delay is introduced by using this approach. Although practical algorithms to compute the Hilbert transform by taking the Fourier transform of the input function, zeroing the negative part of the spectrum and duplicating the positive part, still are not able to overcome this limitation imposed by bandlimiting of the signal. In figure 6 there is an illustration of the effects of the dependence of the Hilbert transform on Nyquist frequency. An impulsive wavelet is generated for different sample rates. The amplitude spectrum is identical inside the common frequency domain of the wavelets. However the extension of the amplitude spectrum to broader frequency bands results in a more accurate representation of the minimum phase wavelet.

The potential impact of the Hilbert transform dependence on the deconvolution methods based on minimum phase assumptions is illustrated in figure 7. In this figure a minimum phase wavelet with a sample rate corresponding to a Nyquist frequency of 1000 Hz is almost perfectly collapsed to a spike by Wiener spiking deconvolution. When the same wavelet is resampled to a bigger sample rate, the resulting ‘spike’ is now time-shifted and phase-rotated.

Aki and Richards (2001) have shown that the earth filter is a causal, physically realizable function endowed with the minimum phase character. They also found an analytical expression for the Hilbert transform of the attenuation function,

$$H\left[\frac{\omega\tau}{2Q}\right] = \frac{\omega}{v(\omega)} - \frac{\omega}{v_\infty} \tag{9}$$

where $v(\omega)$ is the phase velocity of a monochromatic component of the traveling wavelet with frequency ω and v_∞ is the phase velocity when $\omega \rightarrow \infty$. A velocity dispersion relation for $v(\omega)$ is given for example by the expression

$$v(\omega) = v(\omega_0) \left[1 + \frac{1}{\pi Q} \log\left(\frac{\omega}{\omega_0}\right) \right], \tag{10}$$

which matches empirical data inside the range of the seismic frequencies. With the help of equations 9 and 10, a dramatic insight into the impact of using the digital Hilbert transform in correcting attenuation can be obtained. A comparison between the analytical and the digital Hilbert transform of the attenuation function is shown in figure 8. Two remarkable facts can be observed, the digital Hilbert transform differs from the analytical for all the sample rates and the digital Hilbert transform is different for each sample rate. This difference between the two kind of Hilbert transforms has as main consequence the introduction of time shifts and phase rotations between signals obtained from different transforms.

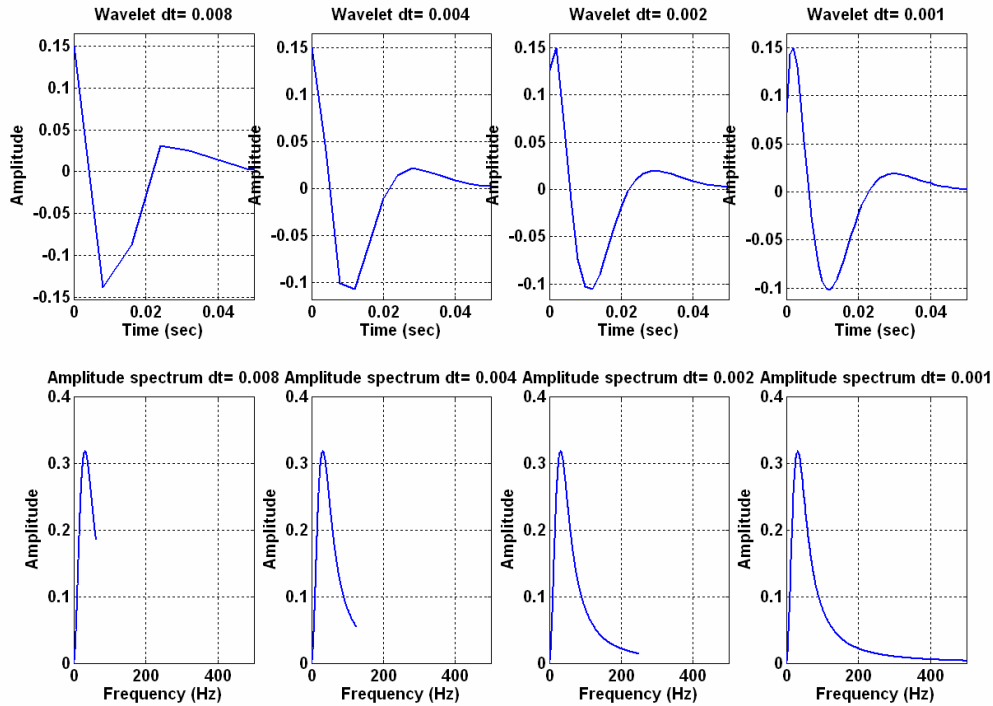


FIG. 6. A minimum phase wavelet representing an impulsive source. The wavelet is generated from its amplitude spectrum using the Hilbert transform. The representation improves for lower sample rates due to the extension of the amplitude spectrum to broader frequency bands.

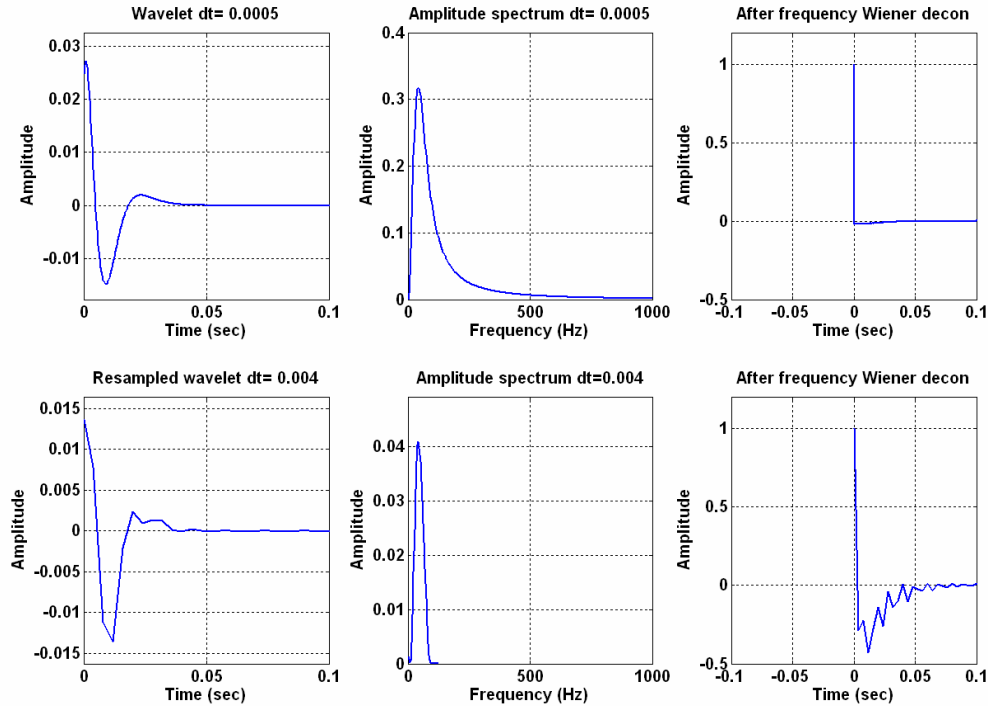


FIG. 7. The impact of the Hilbert transform dependence on the sample rate and Nyquist frequency can be illustrated in this example. The graphs on the top correspond to the Wiener deconvolution (in the frequency domain) of a minimum phase wavelet with a sample rate of 0.5 ms and therefore a Nyquist frequency of 1000 Hz; Wiener deconvolution collapses the wavelet to a good spike at the origin as expected. The graphs on the bottom show the same deconvolution process applied after resampling the wavelet to 4 ms; now the result shows a time shift and a rotation of the resulting spike.

Phase correction in Gabor deconvolution

Velocity dispersion is the cause of the positive drift observed at tying seismic data at a well with a synthetic trace built from its well logs. Digitization of the seismic data imposes a constraint in the maximum frequency recoverable from seismic data; for a typical sample rate of 2 ms, the Nyquist frequency is 250 Hz. Hence the maximum phase velocity for any monochromatic component of a recorded seismic wave will be much lower than the reference velocity used to generate a synthetic seismic trace from well logs. When an algorithm for Gabor deconvolution as described above is applied to seismic data there is a partial restoration of the phase lag due to attenuation, as in the example shown in figures 10 and 13. The restoration is partial because the minimum phase function of the deconvolution operator is built by using a digital Hilbert transform. The phase correction, obtained with the digital Hilbert transform, does not match the phase of the synthetic seismic trace generated from a well log because the digital Hilbert transform is an imperfect estimation, which depends on the sample rate, of the analytical Hilbert transform.

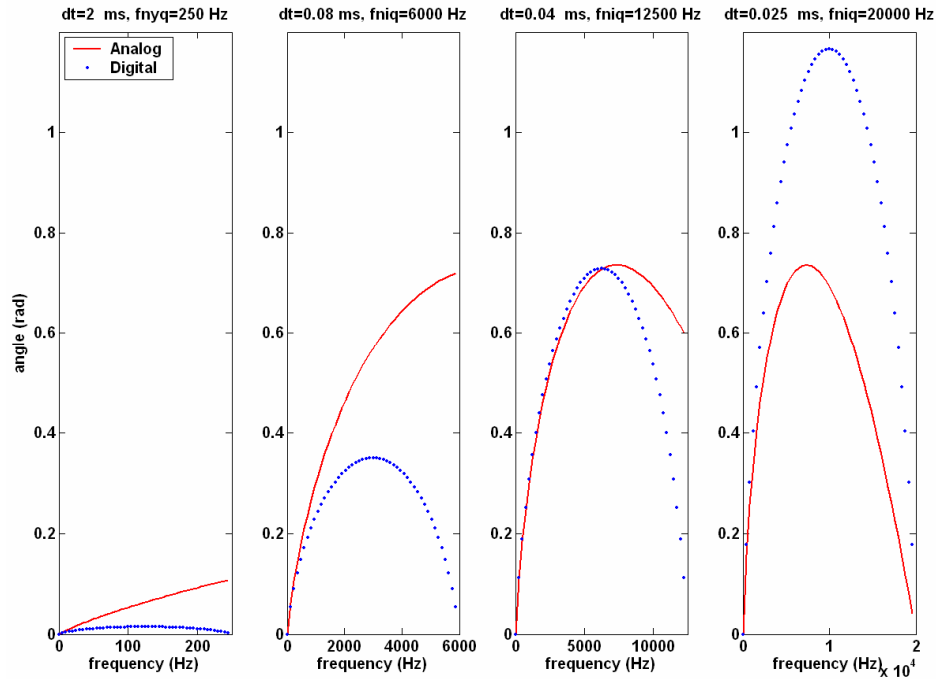


FIG. 8. Minimum phase spectrum estimation for the attenuation impulse response. The minimum phase function can be computed either by analog or by digital Hilbert transform. A better matching between the two transforms is achieved by broadening the spectrum using a higher Nyquist frequency.

Two different methods can be used to correct the remaining phase-shift. A first method consists of adding a time-frequency correction function to the phase operator estimated from the digital Hilbert transform to remove the remaining phase lag. The corrected phase is

$$\varphi_c(t, \omega) = H(\ln|\sigma(\tau, \omega)|) + \frac{t}{Q}(a + b\omega + c\omega^2), \quad (11)$$

where a , b and c depend on the Nyquist frequency and ω_0 . Numerical values for a , b , and c are estimated by regression of a second order polynomial in ω upon the difference between the digitally computed phase and the exact phase expected from constant Q theory.

A reference synthetic nonattenuated trace was used to create an attenuated seismic trace by applying a forward Q filter, using Kjartansson theory, and then convolving the result with a minimum phase wavelet (40 Hz dominant frequency). The reference frequency ω_0 value used is $40,000\pi$ rad/sec. Then Gabor deconvolution was applied to the attenuated traces.

The examples in figures 9 to 12 illustrate phase recovery in Gabor deconvolution for attenuation levels corresponding to $Q=100$. The effects on attenuation on the phase of the recorded signal are shown in figure 9. In figures 9c and 9d can be observed the time-variant phase rotations and phase shifts with respect to the reflectivity, due to the earth

filter action and the convolution with a minimum phase wavelet. In figure 10 the effects of Gabor deconvolution on the phase of the deconvolved trace can be observed. Gabor deconvolution corrects a small portion of the time-shifts when the phase spectrum of the deconvolution operator is computed by the digital Hilbert transform. If the correction term, quadratic in frequency, linear in time and inversely proportional to Q is added up to the digital Hilbert transform a further correction of the phase shifts and the phase rotations can be achieved as shown in figures 11 and 12. A good compensation for the phase-shift can be achieved if a good estimation of Q is available, and just a partial correction is obtained using a poor estimation of Q .

Figures 13 to 15 correspond to an attenuation level of $Q=200$ and illustrate a second method to partially correct the time-shifts. This method is suggested by the variation of the digital Hilbert transform of the attenuation impulse response with the Nyquist frequency, (figure 8). A better matching between the analog and the digital Hilbert transforms can be obtained by resampling the signal. This fact can be used to apply a correction by interpolating the signal to a lower sample rate. In the example shown in figure 15, a partial correction is obtained by resampling to half the original sample rate a signal with an attenuation level corresponding to $Q=200$. This method is conceptually consistent with the theoretical formulation of the problem, but has practical disadvantages such as the increment in the demand of computational resources the fact that the correction is not appreciable for strong attenuation, and the negative effects of noise.

CONCLUSIONS

After applying Gabor deconvolution, a phase lag between the deconvolved trace and a synthetic generated from well logs is observed. This phase difference is attributed to the difference between the analog and the digital Hilbert transform. The minimum phase spectrum of the Gabor deconvolved trace is computed by using the Hilbert transform. The remaining phase-shift can be corrected, if the attenuation is weak, by reconstituting the signal to a smaller sample rate. If an estimation of Q is available an alternative method for correcting the phase can be implemented by adding a function, linear in time and quadratic in frequency, to the digital Hilbert transform.

REFERENCES

- Aki, K., and Richards, P. G., 2002, Quantitative Seismology: Theory and methods. University Science Books.
- Dasgupta, R., and Clark, R. A., 1999, Estimation of Q from seismic surface reflected data: *Geophysics*, **63**, 2120-2128
- Duren, R. E., and Trantham, E. C., 1997, Sensitivity of the dispersion correction to Q error: *Geophysics*, **62**, 288-290.
- Gabor, D., 1946, Theory of communication: *J. Inst. Electr. Eng.*, **93**, 429-457.
- Grossman, J. P., Margrave G. F., Lamoureux M. P., and Aggarwala, R., 2002, Constant- Q wavelet estimation via a Gabor spectral model : CSEG Convention Expanded Abstracts.
- Grossman, J. P., Margrave G. F., and Lamoureux M. P., 2002, Constructing nonuniform Gabor frames from partition of unity. CREWES Research Report, **14**
- Kjartansson, E., 1979, Constant- Q wave propagation and attenuation: *J. Geophysics. Res.*, **84**, 4737-4748
- Hale, D., 1981, An Inverse- Q filter: SEP Report **26**.
- Iliescu, V., and Margrave G. F., 2002, Reflectivity amplitude restoration in Gabor deconvolution: CSEG Convention Expanded Abstracts.

- Iliescu, V., 2002, Seismic signal enhancement using time-frequency transforms. Thesis M.Sc. University of Calgary,
- Margrave, G. F., 1998, Theory of nonstationary linear filtering in the Fourier domain with application to time-variant filtering: *Geophysics*, **63**, 244-259.
- Margrave, G. F., and Lamoureux M. P. 2002, Gabor deconvolution: 2002 CSEG Annual Convention, Calgary, AB.
- Margrave G. F., Dong, L. Gibson, P., Grossman, J. P., Henley D., and Lamoureux M. P., 2003, Gabor Deconvolution: Extending Wiener's Method to nonstationarity: CREWES Research Report, **15**.
- Mertins, A., 1999, *Signal Analysis*: John Wiley and Sons.
- Montana C. A., and Margrave G. F., 2004, Compensating for attenuation by inverse- Q filtering, CREWES Research Report, **16**.
- Robinson, E. A. and Treitel, S., 1980, *Geophysical Signal Analysis*, Prentice-Hall.
- Schoepp, A. R., and Margrave, G. F., 1998, Improving seismic resolution with nonstationary deconvolution: 68th Annual SEG meeting.
- Schoepp, A. R., 1998, Improving seismic resolution with nonstationary deconvolution. Thesis M.Sc. University of Calgary
- Wang, Y., 2002, An stable and efficient approach of inverse- Q filtering: *Geophysics*, **67**, 657-663.

ACKNOWLEDGEMENTS

The authors would like to thank Keith Hirsche from Hampson and Russell for his helpful comments regarding phase and Hilbert transform, and the sponsors of the CREWES Project, the Canadian government funding agencies, NSERC, and MITACS, the CSEG and the Department of Geology and Geophysics University of Calgary for their financial support to this project.

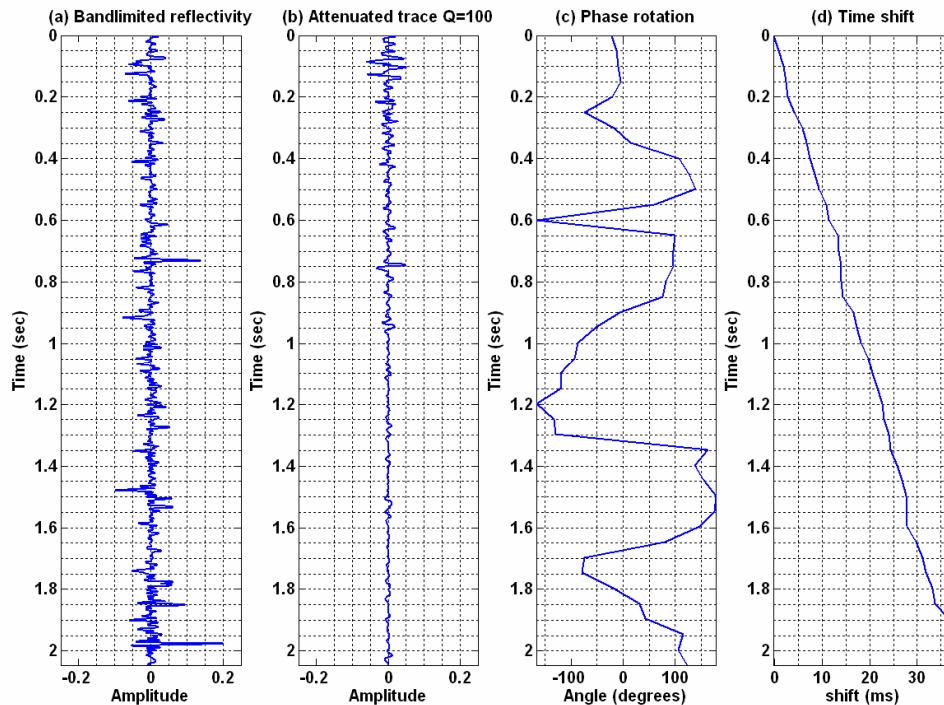


FIG. 9. (a): Bandwidth reflectivity used as reference trace for all the examples in figures 10 to 12. (b): Synthetic attenuated trace created by applying a forward $Q=100$ filter and then by convolving the result with a minimum phase wavelet. (c): Time-variant apparent rotation angle of (b) with respect to trace (a). (d): Time shift between traces (a) and (b).

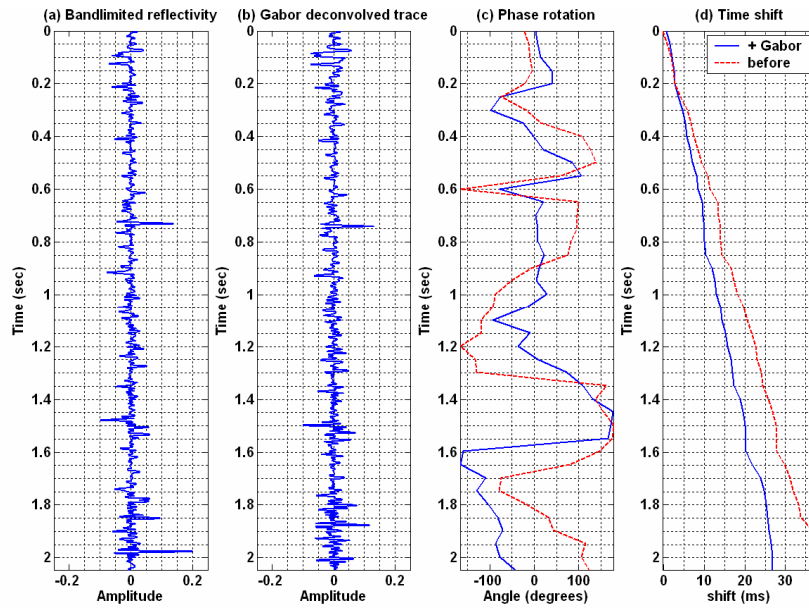


FIG. 10. (a): Same bandwidth reflectivity as in figure 9a. (b): After standard Gabor deconvolution on the attenuated trace in figure 9(b), using equation (5) for the phase (digital Hilbert transform). (c): Remaining phase-shift for trace (a) with respect to the reference trace in figure 3(a). (d): Time-variant apparent rotation angle of trace (b) with respect to trace (a) (continuous line), and comparison with the original before deconvolution of figure 9c (dashed line). (e): Time shift between traces (a) and (b) (continuous line) and comparison with the original before deconvolution (dashed line).

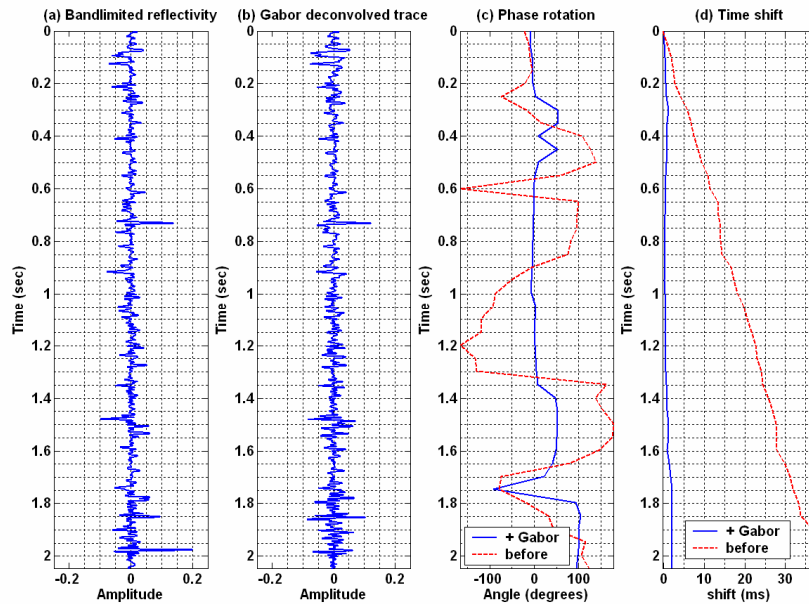


FIG. 11. (a): Same bandwidth reflectivity as in previous two figures, 9a and 10a. (b): After Gabor deconvolution on the attenuated trace in figure 9(b), using equation (11) for the phase (digital Hilbert transform plus correction term), with $Q=100$, (a perfect estimation of Q). (c): Time-variant apparent rotation angle of trace (b) with respect to trace (a) (continuous line), and comparison with the original before deconvolution of figure 9c (dashed line). (d): Time shift between traces (a) and (b) (continuous line) and comparison with the original before deconvolution (dashed line).

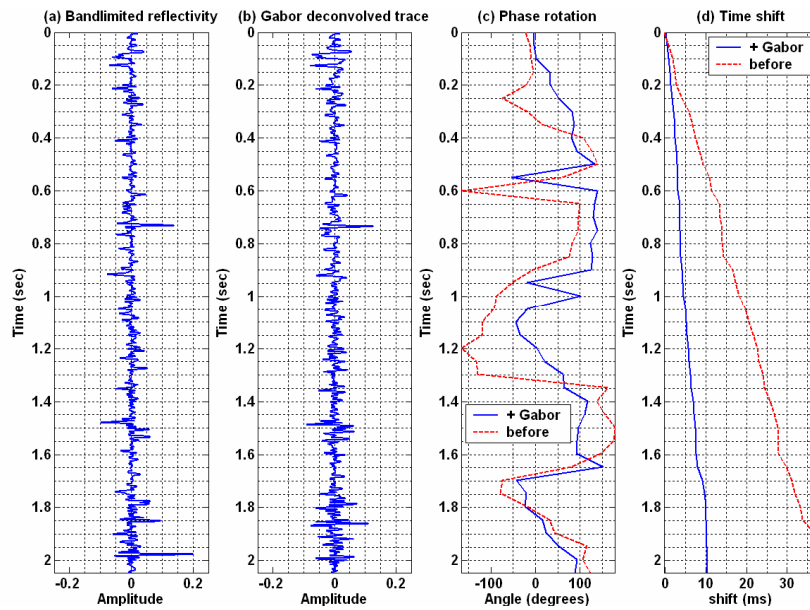


FIG. 12. (a): Same bandwidth reflectivity as in previous three figures, 9a to 11a. (b): After Gabor deconvolution on the attenuated trace in figure 9(b), using equation (11) for the phase (digital Hilbert transform plus correction term), with $Q=150$, (an imperfect estimation of Q). (c): Time-variant apparent rotation angle of trace (b) with respect to trace (a) (continuous line), and comparison with the original before deconvolution of figure 9c (dashed line). (d): Time shift between traces (a) and (b) (continuous line) and comparison with the original before deconvolution (dashed line).

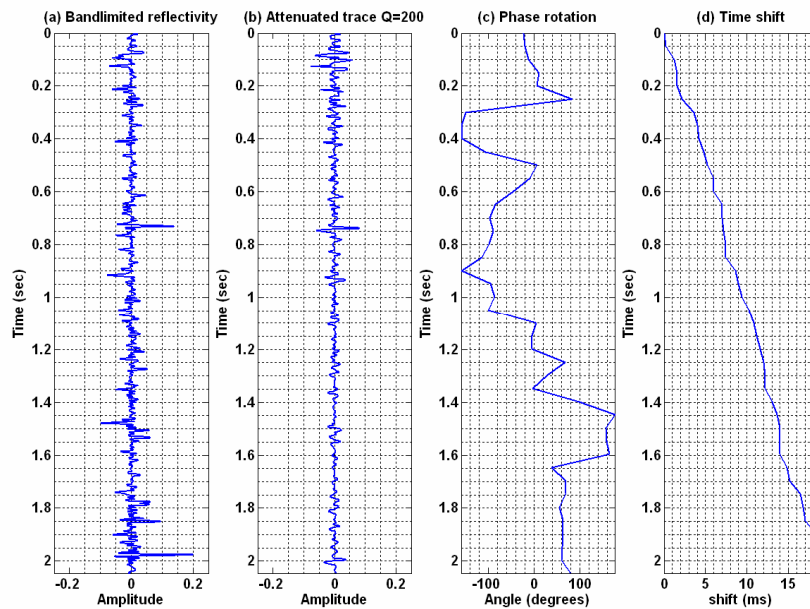


FIG. 13. (a): Bandwidth reflectivity. (b): Synthetic attenuated trace created by applying a forward $Q=200$ filter and then by convolving the result with a minimum phase wavelet. The deconvolution of this trace will be shown in figures 13 and 14. (c): Time-variant apparent rotation angle of trace (b) with respect to trace (a). (d): Time shift between traces (a) and (b).

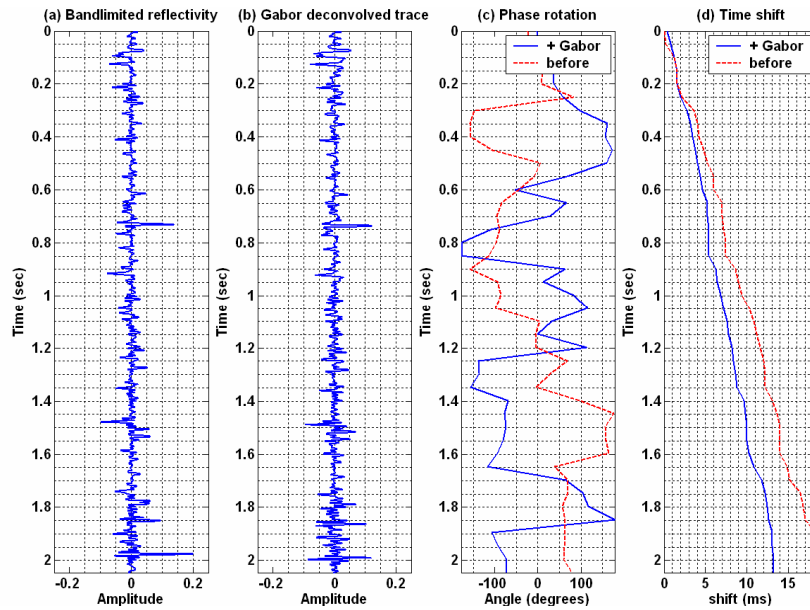


FIG. 14. (a): Bandwidth reflectivity. (b): After Gabor deconvolution on the attenuated trace in figure 13(b), using equation (5) for the phase (digital Hilbert transform). (c): Time-variant apparent rotation angle of trace (b) with respect to trace (a) (continuous line), for comparison the original before deconvolution (figure 13c) is plotted as a dashed line. (d): Time shift between traces (a) and (b) (continuous line) and comparison with the time shift before deconvolution (dashed line).

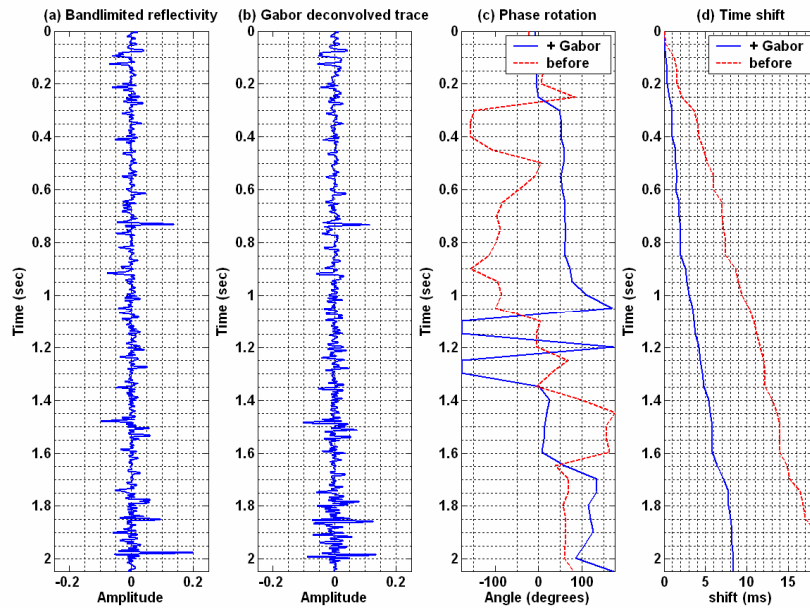


FIG. 15. (a): Bandwidth reflectivity. (b): After Gabor deconvolution on the attenuated trace in figure 13(b), using equation (5) for the phase (digital Hilbert transform), but computing it on the resampled trace to half the sample rate. (c): Time-variant apparent rotation angle of trace (b) with respect to trace (a) (continuous line), for comparison the original before deconvolution (figure 13c) is plotted as a dashed line. (d): Time shift between traces (a) and (b) (continuous line) and comparison with the time shift before deconvolution (dashed line). A partial correction of the time shift is achieved by resampling to compute the digital Hilbert transform.